

No. 347

MAY 2015

# T.W.I.T.T. NEWSLETTER



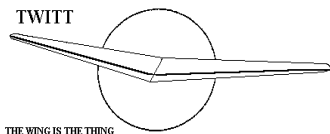
Famed US aerodynamicist R T Jones first suggested in the late 1950s that asymmetrically swept, or oblique, wings offered advantages and calculated that an oblique flying wing offered the lowest supersonic drag. - See more at: <http://www.flightglobal.com/blogs/graham-warwick/2007/08/flying-sideways-1/>

## **T.W.I.T.T.**

The Wing Is The Thing  
P.O. Box 20430  
El Cajon, CA 92021



The number after your name indicates the ending year and month of your current subscription, i.e., **1505** means this is your last issue unless renewed.



**THE WING IS  
THE THING  
(T.W.I.T.T.)**

**T.W.I.T.T.** is a non-profit organization whose membership seeks to promote the research and development of flying wings and other tailless aircraft by providing a forum for the exchange of ideas and experiences on an international basis.

**T.W.I.T.T. Officers:**

**President:** Andy Kecskes (619) 980-9831  
**Treasurer:**  
**Editor:** Andy Kecskes  
**Archivist:** Gavin Slater

The **T.W.I.T.T.** office is located at:  
 Hanger A-4, Gillespie Field, El Cajon, California.  
 Mailing address: P.O. Box 20430  
 El Cajon, CA 92021

(619) 589-1898 (Evenings – Pacific Time)  
**E-Mail:** twitt@pobox.com  
**Internet:** http://www.twitt.org  
 Members only section: ID – 20issues10  
 Password – twittmbr

Subscription Rates: \$20 per year (US)  
 \$30 per year (Foreign)  
 \$23 per year US electronic  
 \$33 per year foreign electronic

Information Packages: \$3.00 (\$4 foreign)  
 (includes one newsletter)

Single Issues of Newsletter: \$1.50 each (US) PP  
 Multiple Back Issues of the newsletter:  
 \$1.00 ea + bulk postage

Foreign mailings: \$0.75 each plus postage

Wt/#Issues	FRG	AUSTRALIA	AFRICA
1oz/1	1.75	1.75	1.00
12oz/12	11.00	12.00	8.00
24oz/24	20.00	22.00	15.00
36oz/36	30.00	32.00	22.00
48oz/48	40.00	42.00	30.00
60oz/60	50.00	53.00	37.00

**PERMISSION IS GRANTED to reproduce this publication or any portion thereof, provided credit is given to the author, publisher & TWITT. If an author disapproves of reproduction, so state in your article.**

**Meetings are held on the third Saturday of every other month (beginning with January), at 1:30 PM, at Hanger A-4, Gillespie Field, El Cajon, California (first row of hangers on the south end of Joe Crosson Drive (#1720), east side of Gillespie or Skid Row for those flying in).**

**TABLE OF CONTENTS**

**President's Corner ..... 1**  
**Tumbling Phenomenon..... 2**  
**Available Plans/Reference Material..... 7**



**PRESIDENT'S CORNER**

This month will finish up the archival piece on tumbling phenomenon started last month. These pages give you the rest of the illustration pages along with the reference materials used for the paper. I hope everyone enjoyed looking at this historic document that I am sure has some controversial concepts based on what we know today.

I was hoping that with the flying season coming to us that there might be some photos and text sent in showing off your winter projects. Unfortunately that hasn't been the case so please give it some thought and send in what you have been doing. I was planning on getting back into radio control so I could experiment with some of the flying wing models that are out there, but it hasn't happened yet due to other projects getting in the way. Maybe later in the year when things calm down a little.

I will dig back into the archives for the June issue. I am sure I can find some other articles of interest that were published by the government or perhaps some unique items from designers like Irv Culver who did a lot of experiments in tailless aircraft over the years.

That's it for this month.

$$q_{ss} \approx -\frac{2V}{\bar{c}} \left( \int_{\theta_0}^{\theta_0 + 2\pi} C_{m\alpha} d\theta + \int_{\theta_0}^{\theta_0 + 2\pi} C_{mq} d\theta \right) \quad (7)$$

The above expression states that for a steady state single degree-of-freedom tumbling condition, the average pitch rate is proportional to the ratio of the areas contained under the static pitching-moment curve and under the pitch-damping curve.

To obtain the static and damping data through  $\pm 180^\circ$  angle-of-attack range required in the mathematical model, tests were conducted in Langley's Spin Tunnel and 30-by 60-Foot Wind Tunnel. A 1/8-scale X-29A model used for rotary-balance testing (figure 10) was tested in the spin tunnel to obtain the necessary static data because the model mounting system was most amenable to the requirements. The 0 to  $90^\circ$  and  $-90^\circ$  angle-of-attack data were obtained with the sting entering the top and bottom of the fuselage, respectively, as is conventionally done during rotary tests. By essentially reversing the model on the sting at each position, the  $90^\circ$  to  $180^\circ$  and  $-90^\circ$  to  $-180^\circ$  quadrants were obtained. Forced-oscillation tests were conducted on a 0.16-scale model in the 30-by 60-foot wind tunnel to determine  $C_{mq}$  through the  $\pm 180^\circ$  angle-of-attack range. Data were measured at an oscillation amplitude of  $\pm 5^\circ$  at a reduced frequency of 0.25.

Figure 11 shows the static pitching-moment data measured for neutral, full nose-up, and full nose-down strake flap deflections with  $\delta_c = 0$  and  $\delta_f$  neutral. The data between  $\pm 45^\circ$  angle of attack exhibit the highly unstable characteristics inherent to this configuration. In the  $\pm 45^\circ$  to  $\pm 140^\circ$  ranges, the data show very stable characteristics such that very large values of pitching moment are generated in the  $\pm 140^\circ$  angle-of-attack regions. Beyond  $\pm 140^\circ$ , the characteristics again break highly unstable. Comparing the three sets of data indicate that the strake flap is most effective in the  $-10^\circ$  to  $75^\circ$  and  $\pm 130^\circ$  to  $\pm 160^\circ$  regions. Plotted in figure 12 are the damping in pitch parameter ( $C_{mq} + C_{m\dot{\alpha}}$ ) obtained in the forced oscillation tests. It is seen that the damping is stable (negative) through most of the angle-of-attack range except in fairly narrow regions centered about  $\alpha = 130^\circ$  and  $\alpha = -120^\circ$ . In contrast to the static data, it was found that strake flap setting has only very minor effects on pitch damping.

Returning to the static pitching-moment data of figure 11 and taking the  $\delta_s = 30^\circ$  data and computing the area contained under the  $C_m$  curve for  $-180^\circ \leq \alpha \leq 180^\circ$  gives a value of  $-.90$  rad. As discussed earlier, this result suggests that this configuration would tend to tumble in the nose-down direction and would not tumble nose-up which is in agreement with the free-tumbling and free-to-pitch results. Further qualitative correlation with the experimental results can be obtained by "walking through" one cycle of the tumbling as

would be predicted by the static data, ignoring damping effects. Starting at  $\alpha = 180^\circ$ , representative of the nose-high launch technique used in the free-tumbling tests, the static pitching-moment data would cause the model to accelerate rapidly in the nose-down direction due to the highly unstable  $C_m$  driving the model into the angle-of-attack region of very large negative values of  $C_m$ . By the time  $C_m$  becomes positive below  $\alpha = 70^\circ$ , the model has built up sufficient kinetic energy to drive it over the positive  $C_m$  "hump" between  $70^\circ$  and  $10^\circ$ . From  $\alpha = 10^\circ$  to  $-80^\circ$ , the model again accelerates in pitch due to the negative values of  $C_m$ . Below  $\alpha = -70^\circ$ , the nose-down rate begins to slow down significantly because of the very large positive  $C_m$  "hump" centered around  $-140^\circ$ . At  $\alpha = -175^\circ$ , the pitch rate has decelerated to its slowest point as  $C_m$  crosses the zero value and the model once again begins to accelerate in the nose down direction at the start of the next cycle. These qualitative motion predictions based on the measured static data agree very well with the experimental results from the free-tumbling and free-to-pitch tests described earlier.

A more exact evaluation of the analytically predicted motions was obtained by inputting the wind-tunnel data into equation (2) and numerically integrating to obtain a time history of the motions. The results obtained for the case described above are shown in figure 13. The calculations were done for a full-scale airplane at  $V = 200$  ft/sec. The computations were started with zero pitch rate and  $\alpha = 180^\circ$  with controls fixed at  $\delta_c = 0$  and  $\delta_s = 30^\circ$ . The time histories show a nose down tumbling motion rapidly developing such that steady-state conditions are achieved after about 5 cycles. The average pitch rate is about  $-130^\circ/\text{sec}$  with the minimum rate of  $-95^\circ/\text{sec}$  occurring at  $\alpha = -180^\circ$  as was observed in the tunnel experiments. Also shown are calculated values of normal and axial accelerations at the pilot station. The results indicate that during tumbling, the pilot will be subjected to a very severe g environment which may be incapacitating as will be discussed in a later section.

Quantitative comparison of the computed and experimental tumbling motions over one cycle for the case discussed above is shown in figure 14. The experimental data were obtained by frame-by-frame reading of movies taken of the model during the free-to-pitch tests and then scaling the time up to full scale. The results show remarkably good agreement between the two sets of data thus providing some confidence in the validity of the mathematical model used in the calculations.

In light of these encouraging results, the analytical model was further exercised to see if it could predict the effect of strake flap setting observed in the experiments. Figure 15 shows computed time histories initiated in a steady-state tumble with  $\delta_c = 0$ ,  $\delta_s = 30^\circ$  as described above. After two complete cycles, the strake flaps were instantaneously moved to the full nose-up position ( $\delta_s = -30^\circ$ ). The data show that the pitch rate immediately began to decrease and the configuration ceased to tumble after completing two more cycles. The results are in good qualitative agreement with the free-to-pitch results discussed earlier.

### Susceptibility to Tumbling

Based on the preliminary experimental and analytical results obtained to date, it appears that the subject configuration may be susceptible to tumbling with the controls fixed. However, for a highly augmented airplane such as the X-29A, the controls are not likely to remain fixed throughout a large amplitude maneuver such as tumbling. Thus at this point in time, it is unknown whether it will be possible for the fully augmented airplane to enter a tumbling condition. Of greater concern, perhaps, are the off-nominal situations involving serious failures in the airplane control system which can lead to conditions which may facilitate entry into a tumble.

A further evaluation of tumble susceptibility of the X-29A is planned for the upcoming radio-controlled drop-model program. In these tests a 0.22-scale dynamic model will be dropped from a helicopter and flown remotely from the ground. The control laws designed for the full-scale airplane will be implemented so that the effect of these laws on tumbling susceptibility can be directly evaluated. This program is expected to get underway in 1985.

The eventual goal of the analytical study is to provide an aerodynamic and mathematical model which will permit piloted simulation of the transition from normal flight to the tumbling conditions. Susceptibility is the key issue for a given configuration and will drive the form of control laws used to provide desired levels of tumble resistance. Based on the limited results obtained to date, it appears that control laws that limit the pitch agility of the airplane will inherently enhance resistance to tumbling. Hard limiters on angle of attack and control laws that limit the attainable pitch rate to "controllable" values would fall into this category. Unfortunately, careful trade-offs versus the desire for high pitch rate capability for nose-pointing agility must be made in designing such systems. Research is currently underway at Langley to develop control laws for highly relaxed stability fighters which combine the desired features of maximum agility and good resistance to pitch departures.

### Flight Test Considerations

Although deliberate tumble flight testing is highly unlikely, preparation for the "worst case" as in high alpha/spin flight testing, will no doubt be required.

### Physiological Considerations

Based on the observed model motions, accelerations on the pilot during tumbling would be violent and could reach levels in excess of 6 g's longitudinally and 4 g's vertically. Centrifuge studies<sup>13,14,15,16</sup> indicate pilot incapacitation and physical injury at these levels. The -Gx ("eyeballs out") and -Gz ("eyeballs up") accelerations are the least documented because they are the most damaging to living subjects. Unfortunately, these accelerations would be present during the tumbling motion. The studies have shown that under such g fields, normal pilot

restraint systems are inadequate, mental and visual functions are impaired, physical manipulation of controls is questionable, and the pilot may suffer from severe pain in the extremities, throbbing headache, petechial hemorrhages, edematous eyelids, and congested and hemorrhagic conjunctivae.

### Pilot Escape Considerations

The cited centrifuge studies have demonstrated that pilot egress will be severely compromised by these unusual g environment. The generally inadequate restraint systems permit body positions likely to cause injury during ejection. The use of helmet restraints is shown to be both necessary and very dangerous. Above -3Gx pilots are generally unable to reach face-curtain ejection handles. Aside from pilot incapacitation, the ability of an escape system to function properly under tumbling conditions must be determined.

### Emergency Recovery

For flight testing at extreme angles of attack, the test vehicle is usually provided with an emergency spin recovery parachute. Emergency tumble recovery has not yet been addressed in these studies, however, the typical spin chute (figure 16) would have a high probability of tangling with the aircraft if deployed during a tumble. Wing-tip parachutes (figure 17), simultaneously deployed in pairs, were effective in early tumble tests<sup>2</sup>, but their effectiveness has not been established for the X-29A. The rigid towline system (figure 18) discussed in reference 17 might be implemented to provide both spin and tumble recovery.

### Instrumentation

Tumbling presents some interesting problems for flight-test data acquisition, including angle-of-attack measurement through 360° of rotation and air data measurement during the "backwards" portions of the trajectory. Linear accelerations at the pilot's station will be of great importance and angular acceleration measurements would be very useful. A greatly expanded maximum range for pitch rate measurement is mandatory.

### Concluding Remarks

The continuing drive for increased agility and maneuverability in high performance aircraft has produced design trends which include relaxed static stability and the elimination of aft-mounted horizontal tails. These design trends have reestablished the tumbling phenomenon as a concern for flight mechanics. Recent model tests on the X-29A configuration have demonstrated the existence of tumbling for such designs, and have prompted experimental and analytical investigations of tumbling. The results of the continuing research will be used to provide aerodynamic and flight control guidelines to designers of future high performance configurations.

### References

1. Chambers, J. R. and Grafton, S. B.: "Aerodynamic Characteristics of Airplanes at High Angles of Attack"; NASA TM 74097, December 1977.

2. Stone, R. W., Jr. and Bryant, R. L.: "Summary of Results of Tumbling Investigations Made in the Langley 20-Foot Free-Spinning Tunnel on 14 Dynamic Models"; NACA RM L8J28, December 1948.
3. Klinar, W. J.: "Free-Spinning and Tumbling Tests of a 1/16-Scale Model of the McDonnell XP-85 Airplane"; NACA RM No. L7C10, March 1947.
4. Stone, R. W., Jr. and Daughtridge, L. T., Jr.: "Free-Spinning, Longitudinal-Trim, and Tumbling Tests of 1/17-Scale Models of Corneliuss XFC-1 Glider"; NACA MR No. L5K21, 1945.
5. Kamm, R. W. and Snyder, T. L.: "Spin and Tumbling Tests of a 1/16-Scale Model of the Avion XP-79 Airplane in the Langley Spin Tunnel"; NACA MR No. L5E23, June 1945.
6. Bryant, R. L.: "Longitudinal Trim and Tumble Characteristics of a 0.57 Scale Model of the Chance Vought XF7U-1 Airplane"; NACA RM No. SL8P14, July 1948.
7. Gale, L. J.; Jones, I. P.; and Wilson, J. H.: "An Investigation of the Spin, Recovery, and Tumbling Characteristics of a 1/20-Scale Model of the Northrop X-4 Airplane". NACA RM L9K28, January 1950.
8. Bowman, J. S., Jr.: "Concluding Report of Free-Spinning Tumbling, and Recovery Characteristics of a 1/18-Scale Model of the Ryan X-13 Airplane"; NACA RM SL 57D11, May 1957.
9. Libbey, C. E. and Johnson, J. L., Jr.: "Stalling and Tumbling of a Radio-Controlled Parawing Airplane Model"; NASA TN D-2291; July 1964.
10. Wolowicz, C. M., Bowman, J. S., Jr., and Gilbert, W. P.: "Similitude Requirements and Scaling Relationships as Applied to Model Testing"; NASA Technical Paper 1435, August 1979.
11. Smith, A. M. O.: "On the Motion of a Tumbling Body"; Douglas Aircraft Co., Inc. December 1951.
12. Nelhouse, A. I.; Klinar, W. J.; and Scher, S. M.: "Status of Spin Research for Recent Airplane Designs"; NASA TR R-57 1960. (Supersedes NACA RM L97F12.)
13. Fraser, T. M.: "Human Response to Sustained Acceleration"; NASA SP-103, 1966.
14. Van Patten, R. E.; Frazier, J. W.; Luciani, R. J.; Rogers, D. B.; Roark, M.; and Abrams, R.: "Observations on Human Exposures to Combined - Gx/+ Gz Acceleration Fields"; AFAMRL-TR-81-17, July 1981.
15. Snyder, R. Z.: "A3J-1 Spin Simulation Program on the Navy Human Centrifuge"; NADC-MA-6104, March 1961.
16. Miller, C. O.: "Evaluation of Transverse Acceleration (Rear to Front) Utilizing

Conventional and Special Restraint Gear"; Chance Vought Aircraft Report No. 10816; February 1957.

17. Whipple, Raymond D.: "Current Perspectives on Emergency Spin Recovery Systems". Proceedings of the Society of Flight Test Engineers 13th Annual Symposium, September 1982.
18. Lee, H. A.: "Free-Spinning and Tumbling Characteristics of a 1/20-Scale Model of the Douglas XF4D-1 Airplane as Determined in the Langley 20-Foot Free-Spinning Tunnel"; NACA D. E. 346, December 1950.
19. Bryant, R. L.: "Preliminary Empirical Design Requirements for the Prevention of Tumbling of Airplanes Having No Horizontal Tails"; NACA RM L50H23, October 1950.
20. Murri, Daniel G.; Nguyen, Luat T.; and Grafton, Sue B.: "Wind Tunnel Free-Flight Investigation of a Model of a Forward-Swept Wing Fighter Configuration". NASA TP-2230, February 1984.

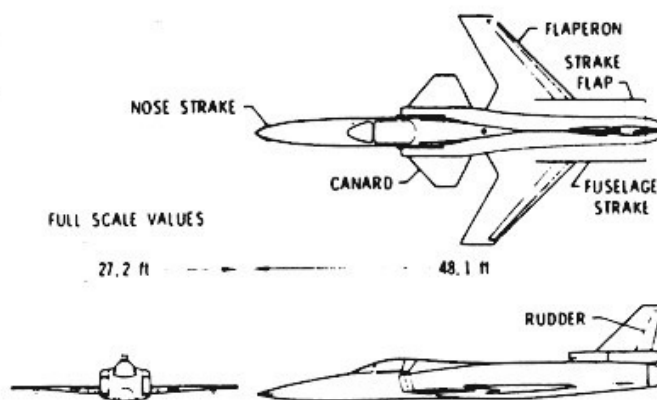


Figure 1.- Three-view drawing of the X-29A configuration.

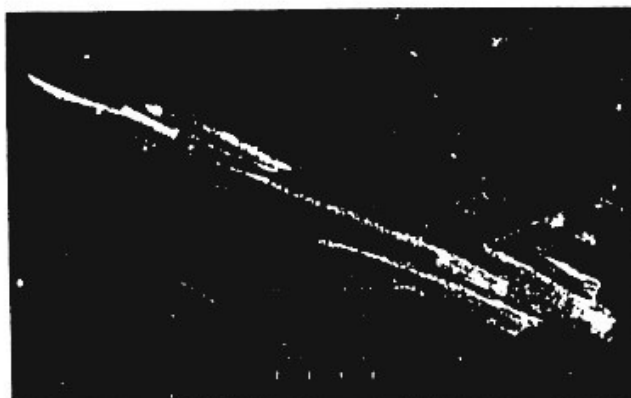


Figure 2.- Photograph of the 1/25-scale model of the X-29A.

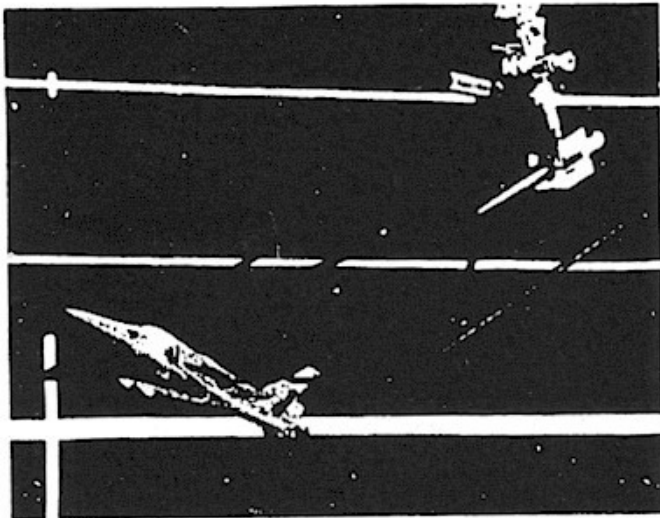


Figure 9.- X-29A model mounted on free-to-pitch rig.

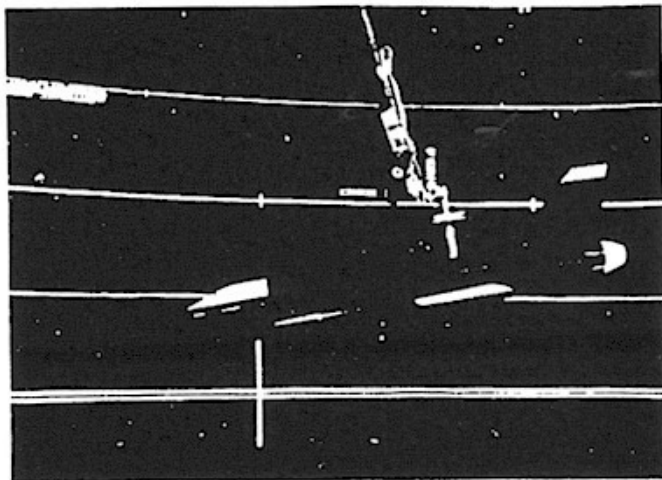


Figure 10.- 1/8-Scale model of X-29A on rotary balance.

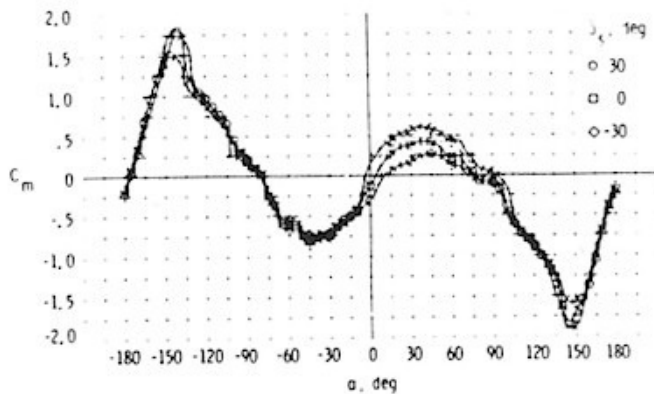


Figure 11.- Pitching moment variation with angle of attack, effect of strake flap setting.

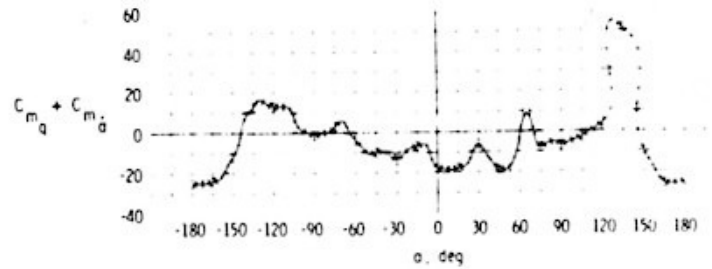


Figure 12.- Damping in pitch parameter ( $C_{m\dot{q}} + C_{mq}$ ) variation with angle of attack.

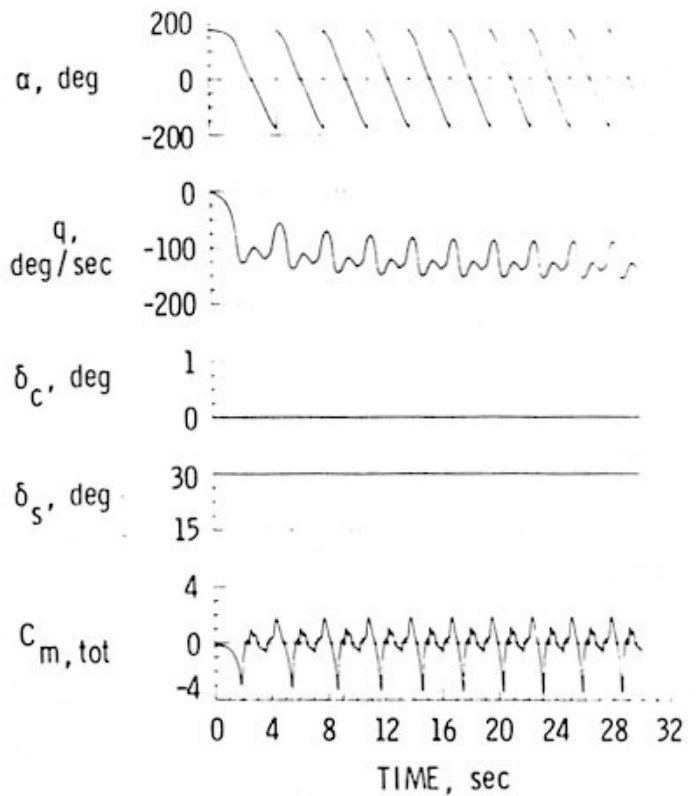
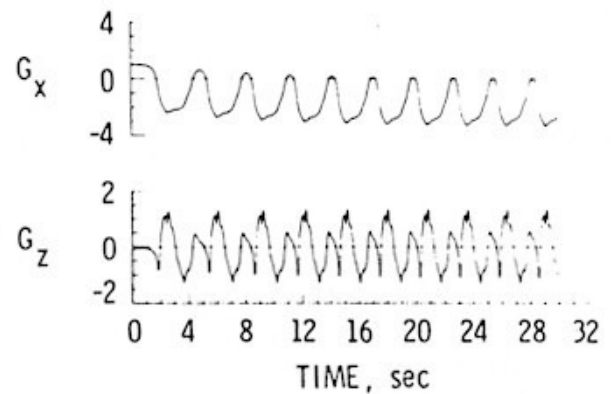


Figure 13.- Time history of a computed tumbling motion.



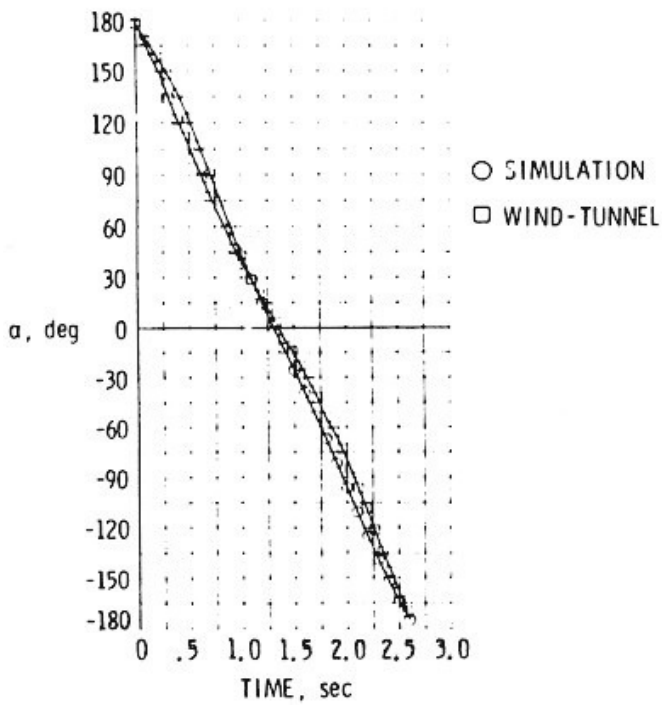


Figure 14.- Comparison of computed and experimental data.

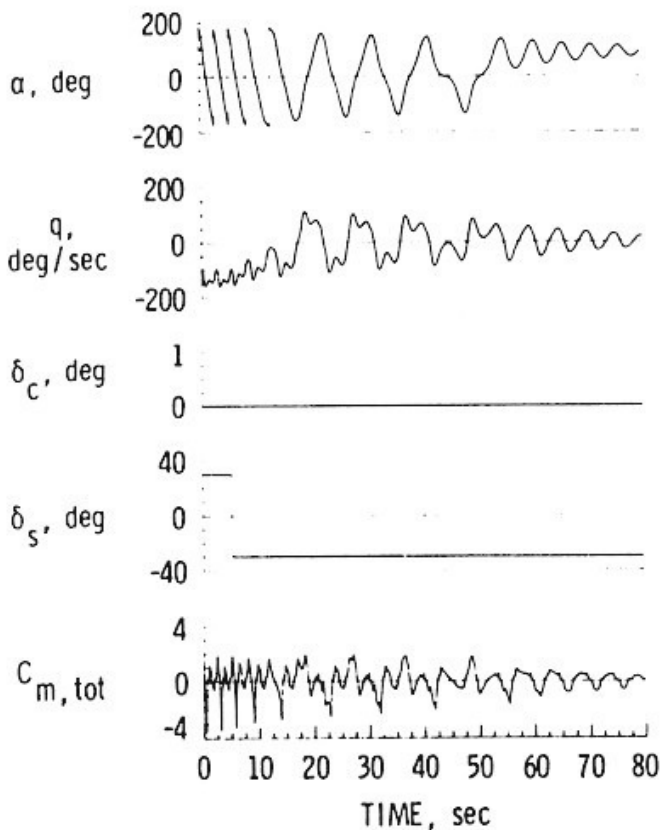


Figure 15.- Time history of a computed recovery from tumbling.

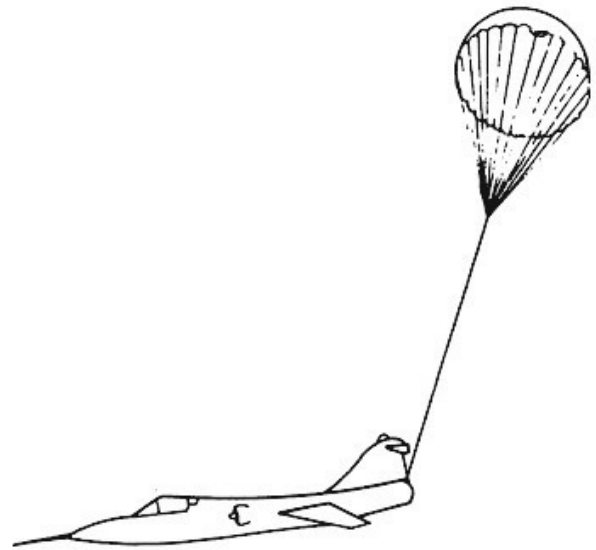


Figure 16.- Conventional anti-spin parachute system.

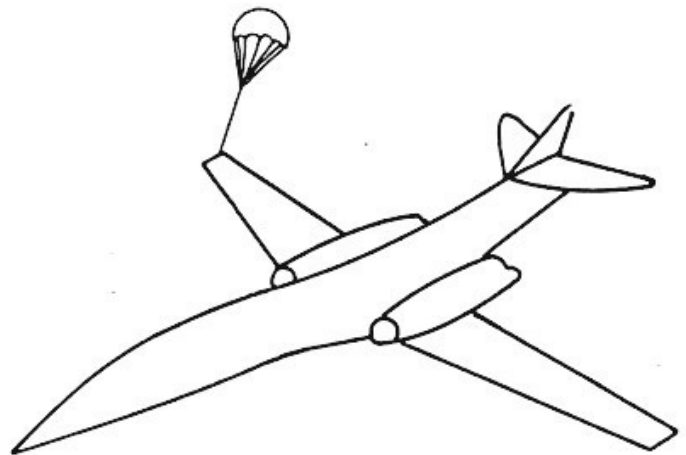


Figure 17.- Wing-tip mounted anti-spin parachute system.

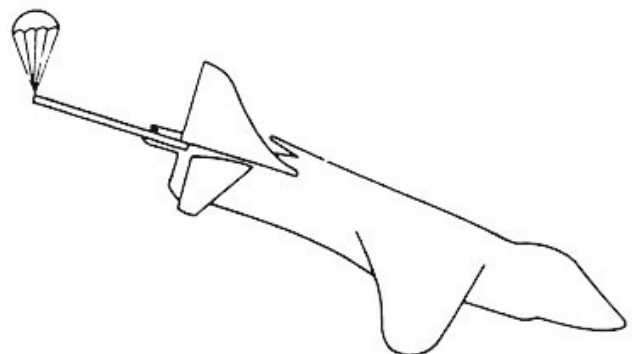


Figure 18.- Rigid-towline anti-spin parachute system.

